Proceedings of ASME Turbo Expo 2010: Power for Land, Sea, and Air
GT2010
June 14-18, 2010, Glasgow, UK

GT2010-22532

A CREEP RUPTURE TIME MODEL FOR ANISOTROPIC CREEP-DAMAGE OF TRANSVERSELY-ISOTROPIC MATERIALS

Calvin M. Stewart
Department of Mechanical, Materials, & Aerospace Engineering, University of Central Florida
Orlando, FL USA 32816-2450

Ali P. Gordon
Department of Mechanical, Materials, & Aerospace Engineering, University of Central Florida
Orlando, FL USA 32816-2450

ABSTRACT

Anisotropic creep-damage modeling has become an increasingly important prediction technique in both the aerospace and industrial gas turbine industries. The introduction of tensorial damage mechanics formulations in modeling tertiary creep behavior has lead to improved predictions of the creep strain that develops due to anisotropic grain structures and the induced anisotropy that occurs with intergranular damage. A number of isotropic creep-damage rupture time prediction models have been developed in literature; however, few rupture time prediction models for tensorial anisotropic creep-damage are available. In this paper, a rupture time model for anisotropic creep-damage of transversely isotropic materials is derived. Comparison with the Larson-Miller parameter, Monkman-Grant relation, and Kachanov-Rabotnov continuum damage mechanics (CDM) approach shows improved creep rupture time predictions for multiaxial conditions and material rotations. A parametric study of the rupture time predicted under various states of equivalent stress and material orientations is performed to demonstrate the robustness of the new formulation.

1. INTRODUCTION

Gas turbine components undergo a myriad of thermal and mechanical loads and typically exhibit creep deformation. This plastic deformation reduces the operational lifetime of components and must be accounted for. Components of particular importance are gas turbine blades. Turbine blades experience high temperatures, fuel and air contamination (in marine turbine chlorine due to salt water), and foreign object damage (FOD) within a corrosive environment. High stress due to centrifugal forces, dynamic flutter and vibrations, flexural stresses due to combustion gases interfacing with blade surface area, and thermal gradient induced thermal stresses impart a complex state of stress on gas turbine blades [1]. Stress concentrations near the blade root are the frequent location of crack initiation. Fatigue, creep damage and the interactions of both are the principal cause of microstructural damage leading to eventual failure [2]. In the case of IGT turbine blades where the cycle duration and maintenance intervals can in the thousands of hours, DS materials have been implemented to minimize intergranular (brittle) creep cracking by alignment of longitudinal grains (L) with the first principal stress direction [3]. However, the regulation of thrust to produce lower or higher power output and the regular fluctuations in combustion exit exhaust velocity coupled with the existence of inherit vibration issues can result in a first principal stress direction not aligned with the enhanced (L) material orientation.

Creep rupture prediction approaches such as Monkman-Grant and the Larson-Miller Parameter are useful, but are based strictly around uniaxial tensile tests. The rupture time of a specimen under a multiaxial state of stress cannot be accurately predicted. The orientation-dependent creep damage behavior of transversely-isotropic materials can be determined by machining a specimen at the desire orientation and implementing the creep rupture prediction approach. None of the approaches allow for both multiaxial states of stress and rupture prediction at arbitrary material orientations.

Isotropic creep-damage formulations are based around an equivalent stress such as von Mises, or Hill's potential which includes all stress contributions. Unfortunately, these isotropic-scalar formulations are unable to model the orientation-dependence of transversely-isotropic materials.

Creep-damage constitutive modeling efforts for creep deformation of anisotropic materials have been limited. Few models have been developed, optimized, and actually compared with creep test data. In the case of transversely-isotropic turbine blade materials with induced anisotropic damage, no models currently exist.

A number of creep rupture prediction models are implemented in industry; however, no models have been developed that are capable of predicting the creep rupture time under complex states of stress and arbitrarily materials rotations of a transversely-isotropic material.

In this paper, the Larson-Miller, Monkman-Grant, and Kachanov-Rabotnov rupture time prediction approaches are compared with a new rupture time prediction approach for the transversely-isotropic subject material DS GTD-111.

2. CREEP RUPTURE TIME MODELS

2.1. Larson-Miller Parameter

One of the earliest creep rupture prediction approaches was produced by Larson and Miller [4]. This approach is based on a time-temperature relationship as follows

$$LMP = T\left(\log t_r + K_1\right) \tag{1}$$

where T is temperature in kelvin, t_r is rupture time, K_1 is a constant, and LMP is the Larson-Miller parameter. For metals, K_1 is typically set to 20. The LMP parameter can be determined from stress and the creep strain rate [5]. The Larson-Miller method requires a suitable set of creep deformation tests to be performed up to rupture. A plot of stress versus LMP is created and the K_1 constant is adjusted until the LMP parameter is described as a logarithm of stress. Once the K_1 constant has been determined, rupture time predictions can be produced by using the known T and LMP from the applied boundary conditions. A regression equation for LMP based on the stress versus LMP plot can be easily created. Rupture predictions can then be produced by rearranged the Larson-Miller relation into the following form

$$t_r = 10^{\frac{LMP - T\cdot K_1}{T}} \tag{2}$$

This method has been used consistently with Ni-based superalloys [6]. Ibanez and colleagues produced LMP predictions for DS GTD-111 [7]. It should be noted that rupture predictions should be made within the upper and lower bound of stress and temperature found in available creep rupture experiments. The material may exhibit a behavior that is not captured within available experiments.

2.2. Monkman-Grant

The classical approach to modeling the secondary creep behavior for materials is the Norton power law for secondary creep [8]

$$\dot{\varepsilon}_{cr} = \frac{d\varepsilon_{cr}}{dt} = A\bar{\sigma}^n \tag{3}$$

where A and n are the secondary creep constants, and $\bar{\sigma}$ is an equivalent stress. Typical the von Mises equivalent stress which is both isotropic and pressure insensitive is used of the form

$$\begin{aligned} \sigma_H &= \sigma_{kk}/3 \\ \mathbf{S}_{ij} &= \boldsymbol{\sigma}_{ij} - \sigma_H \\ \sigma_{vm} &= \sqrt{\frac{3}{2}\mathbf{S}_{ij}\mathbf{S}_{ij}} \end{aligned} \tag{4}$$

where σ_H is the hydrostatic (mean) stress and $\mathbf{S}$ is the deviatoric stress tensor. For anisotropic materials, the well known Hill's anisotropic equivalent stress is implemented of the form

$$\begin{aligned} \sigma_{\text{Hill}} &= \sqrt{\mathbf{s}^T\mathbf{M}\mathbf{s}} \\ \mathbf{s} &= VEC\left(\boldsymbol{\sigma}\right) \\ \mathbf{M} &= \begin{bmatrix} G+H & -H & -G & 0 & 0 & 0 \\ -H & F+H & -F & 0 & 0 & 0 \\ -G & -F & F+G & 0 & 0 & 0 \\ 0 & 0 & 0 & 2N & 0 & 0 \\ 0 & 0 & 0 & 0 & 2L & 0 \\ 0 & 0 & 0 & 0 & 0 & 2M \end{bmatrix} \end{aligned} \tag{5}$$

where $\mathbf{s}$ is the vector form of the Cauchy stress tensor, $\boldsymbol{\sigma}$, and $\mathbf{M}$ is the Hill compliance tensor [9] consisting of the F, G, H, L, M, and N unitless material constants that can be obtained from creep tests [10]. Hill's equivalent stress reverts to von Mises when

$$\begin{aligned} F = G = H &= \frac{1}{2} \\ L = M = N &= \frac{3}{2} \end{aligned} \tag{6}$$

The Norton power law is sometimes referred to as the Norton-Bailey law. The secondary creep constants A and n exhibit temperature-dependence. Stress provides a substantial contribution to the creep strain rate as the n secondary creep constant is an exponent of stress.

Dorn [11] suggested that temperature contributions can be accounted for by replacing the A constant with an Arrhenius equation

$$\dot{\varepsilon}_{cr} = \frac{d\varepsilon_{cr}}{dt} = B\bar{\sigma}^n \exp\left(\frac{-Q_{cr}}{RT}\right) \tag{7}$$

where B is the pre-exponential factor in units $MPa^{-1}\ hr^{-1}$, Q_{cr} is the apparent activation energy for creep deformation in units $J\ mol^{-1}$, R is the universal gas constant 8.314 $J\ mol^{-1}\ K$, and T is

temperature in units Kelvin. Using this equation, stress and temperature contributions to the strain rate are obtained. The secondary creep constants can be determined from uniaxial creep tests by rearranged Eq. (7) into the following form

$$\ln \dot{\varepsilon}_{\min} = \ln B + n \ln \bar{\sigma} + \frac{-Q_{cr}}{RT} \tag{8}$$

where the creep strain rate $\dot{\varepsilon}_{cr}$ is replaced with the minimum creep strain rate $\dot{\varepsilon}_{\min}$. Plotting the log of the minimum creep strain versus $1/T$, the apparent activation energy of creep, Q_{cr}, can be determined as the slope. Plotting the log of the minimum creep strain versus von Mises equivalent stress, the secondary creep constant, n, can be determined as the slope.

Monkman and Grant [12] observed that creep rupture can be predicted for many alloy systems using the following expression

$$\log(t_r) + m\log(\dot{\varepsilon}_{\min}) = k_{MG} \tag{9}$$

where $\dot{\varepsilon}_{\min}$ is the minimum creep strain rate, t_r is the creep rupture time, m is a constant, and k_{MG} is the referred to as the Monkman-Grant constant. For some materials m is assumed equal to unity furnishes a simplified form of Eq. (9) expressed as

$$\dot{\varepsilon}_{\min} t_r = k_{MG} \tag{10}$$

Previous studies show that the Monkman-Grant relationship produces accurate rupture time predictions for various DS Ni-based superalloys [7,13]. This formulation can be further extended by replacing the minimum creep strain rate in the Monkman-Grant expression Eq. (9) with the temperature-dependent Norton power law for secondary creep Eq. (7) thus both temperature and stress are related to creep rupture time by the Monkman-Grant constant. The Monkman-Grant method requires a suitable set of creep deformation tests to be performed up to rupture. Using the known set of minimum creep strain rate, $\dot{\varepsilon}_{\min}$ and rupture time, t_r optimization provides suitable m and K_{MG} constants.

Rupture predictions can then be produced by rearranged the Monkman-Grant relation into the following form

$$t_r = \frac{10^{k_{MG}}}{\dot{\varepsilon}_{\min}{}^{m}} \tag{11}$$

Again, it should be noted that rupture predictions should be made within the upper and lower bound of stress and temperature found in available creep rupture experiments.

2.3. Kachanov-Rabotnov Isotropic CDM Approach

To account for the tertiary creep damage behavior of materials, Kachanov [14] and Rabotnov [15] developed a Continuum Damage Mechanics (CDM) based isotropic creep-damage formulation. Damage is an all inclusive non-recoverable accumulation that exhibits the same dependences as creep deformation: material behavior (i.e., creep constants), temperature, time, and stress. Generally, damage is considered to be in continuum, (i.e., homogenous thought a body) thereby the expression *continuum damage mechanics* (CDM) is used.

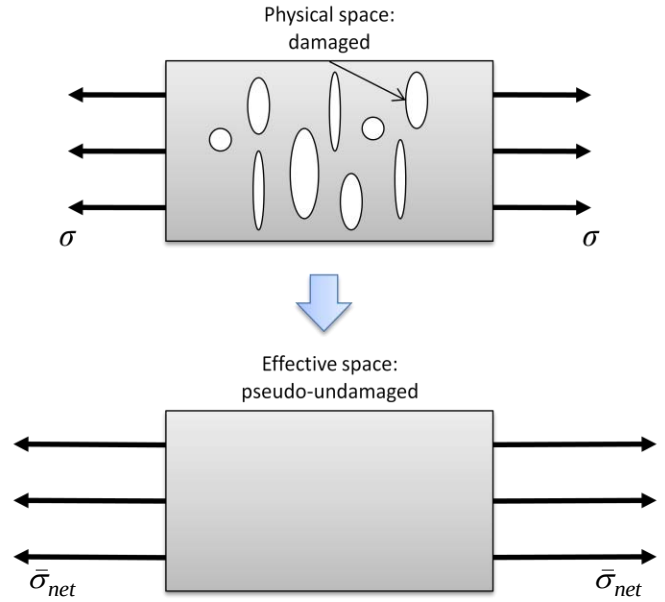

Figure 1 - Schematic demonstrating the concept of a physical and effective space

The concept of scalar-valued damage evolution expressed as $f(\sigma, T, \omega)$ is introduced where σ is uniaxial stress, ω is the current state damage. Damage is coupled within the creep strain rate via current damage and is expressed as $g(\sigma, T, \omega)$. Within the creep strain equation, there arises a net/effective stress which relates the physical space of damage where the presence of microstructural defects reduces creep strength, to an effective space, where microstructural creep damage is replaced with an effective increase in the applied stress, as conceptualized in Figure 1. While the figure idealized damage as due to voids, damage actually includes all microstructure evolution leading to failure.

The Kachanov [14] and Rabotnov [15] proposed equations for the creep rate and damage evolution are as follows

$$\dot{\varepsilon}_{cr} = \frac{d\varepsilon_{cr}}{dt} = A\left(\frac{\bar{\sigma}}{1-\omega}\right)^{n} \tag{12}$$

$$\dot{\omega} = \frac{d\omega}{dt} = \frac{M\bar{\sigma}^{\chi}}{(1-\omega)^{\phi}} \tag{13}$$

where the creep strain rate is equal to Norton's power law for secondary, Eq. (3), with the same associated A and n constants, $\bar{\sigma}$ is von Mises stress, and M, χ, and ϕ are tertiary creep damage constants. Numerous authors have developed specialized formulations based on this fundamental formulation [16-21]. These formulations based around von

Mises equivalent stress, have also been generalized for multiaxial states of stress in isotropic materials using elastic compliance tensors and the stress deviator [22]. An isochoric creep behavior (incompressibility) is assumed.

Rupture time predictions can be easily arrived at using damage evolution Eq. (13). Separation of variables, integration, and simplification furnishes the following

$$t_r = \left[1-\left(1-\omega_{cr}\right)^{\phi+1}\right]\left[\left(\phi+1\right)M\bar{\sigma}_r^{\chi}\right]^{-1} \tag{14}$$

where ω_{cr} is critical damage at which rupture occurs. Typically, ω_{cr} is assumed to be unity.

3. New Transversely-Isotropic CDM Approach

A new model developed by the authors is an extension of the isotropic Kachanov-Rabotnov creep damage model [14,15]. The influence of the state of damage, $\boldsymbol{\omega}$ is accounted for via the effective (net) stress tensor, $\tilde{\boldsymbol{\sigma}}$. The Murakami and Ohno [23] symmetric effective (net) stress, $\tilde{\boldsymbol{\sigma}}$ and a simplified damage applied, $\boldsymbol{\Omega}$ are applied

$$\begin{aligned}\boldsymbol{\Omega} &= \left(\mathbf{I}-\boldsymbol{\omega}\right)^{-1}\\ \tilde{\boldsymbol{\sigma}} &= \frac{1}{2}\left(\boldsymbol{\sigma}\boldsymbol{\Omega}+\boldsymbol{\Omega}\boldsymbol{\sigma}\right)\end{aligned} \tag{15}$$

where $\boldsymbol{\sigma}$ is the Cauchy stress tensor and $\boldsymbol{\Omega}$ is damage applied. Damage is represented by multiple principal damage variables due to induced anisotropy [24,25] in the form of a damage tensor

$$\omega = \begin{bmatrix}\omega_1 & 0 & 0\\ 0 & \omega_2 & 0\\ 0 & 0 & \omega_3\end{bmatrix} \tag{16}$$

where each term of damage corresponds to the orthogonal planes of a material.

Creep damage anisotropy is introduced via two damage constant tensors. The tertiary creep damage constants are generalized into a vector (6x1) form using the anisotropic Hill potential theory transformed into damage constant tensors (3x3). The vectors take the following form

$$\begin{aligned}\mathbf{b}^R &= M_{aniso}\sigma_{Hillb}^{\chi_{aniso}}\frac{\mathbf{M}_b\mathbf{s}_p}{\sigma_{Hillb}} & \boldsymbol{\lambda}^R &= \phi_{aniso}\frac{\mathbf{M}_\lambda\mathbf{s}_p}{\sigma_{Hill\lambda}}\\ \mathbf{b} &= \mathrm{ABS}\left(\mathbf{b}^R\right) & \boldsymbol{\lambda} &= \mathrm{ABS}\left(\boldsymbol{\lambda}^R\right)\\ \mathbf{b} &= \mathrm{VEC}\left(\mathbf{B}\right) & \boldsymbol{\lambda} &= \mathrm{VEC}\left(\boldsymbol{\Phi}\right)\end{aligned} \tag{17}$$

where M_{aniso}, χ_{aniso}, and ϕ_{aniso} are tertiary creep damage constants and $\mathbf{s}_p$ is the vector form of the principal stress. The ABS function, represents an element-wise absolute value of the argument vector and is introduced to enforce damage accumulation. The principal stress vector can be found solving the following

$$\begin{aligned}&\det\left[\boldsymbol{\sigma}-\sigma_n\mathbf{I}\right]=0\\ &\boldsymbol{\sigma}_p = \begin{bmatrix}\sigma_{n,1} & 0 & 0\\ 0 & \sigma_{n,2} & 0\\ 0 & 0 & \sigma_{n,3}\end{bmatrix}\\ &\mathbf{s}_p = VEC\left(\boldsymbol{\sigma}_p\right)\end{aligned} \tag{18}$$

where $\boldsymbol{\sigma}_p$ is a tensor of the principal stress where the subscripts (1,2,3) denote the orthogonal material planes. The stresses σ_{Hill}, σ_{Hillb}, and $\sigma_{\mathrm{Hill}\lambda}$ are forms of Hill equivalent stress defined as

$$\begin{aligned}\sigma_{\mathrm{Hill}} &= \sqrt{\mathbf{s}^T\mathbf{M}\mathbf{s}}\\ \sigma_{\mathrm{Hillb}} &= \sqrt{\mathbf{s}_p{}^T\mathbf{M}_b\mathbf{s}_p}\\ \sigma_{\mathrm{Hill}\lambda} &= \sqrt{\mathbf{s}_p{}^T\mathbf{M}_\lambda\mathbf{s}_p}\\ \mathbf{s} &= VEC\left(\boldsymbol{\sigma}\right)\end{aligned} \tag{19}$$

where $\mathbf{s}$ is the vector form of the Cauchy stress tensor, $\boldsymbol{\sigma}$ and $\mathbf{M}$ is the Hill compliance tensor [9], Eq. (5), consisting of the *F*, *G*, *H*, *L*, *M*, and *N* unitless material constants that can be obtained from creep tests [10]. The damage constant vectors, $\mathbf{b}$ (hr^{-1}) and $\boldsymbol{\lambda}$ (unitless), require a unique Hill compliance tensor, $\mathbf{M}_{\mathrm{b}}$ and $\mathbf{M}_{\lambda}$, respectively. Each compliance tensor requires 6 unitless material constants that can be determined analytically.

In the isotropic damage formulation Eq. (13), it is observed that previous scalar-valued damage is related by $\left(1-\omega\right)^{-\phi}$. An equivalent tensor form is produced by use of the elementwise Schur (or Hadamard) power of the damage applied tensor, $\boldsymbol{\Omega}$ and the rotated damage constant tensor, $\boldsymbol{\Phi}$ as follows

$$\begin{aligned}\mathbf{D} &= \overrightarrow{\boldsymbol{\Omega}^{\boldsymbol{\Phi}}} = \boldsymbol{\Omega}^{\circ\left(\boldsymbol{\Phi}\right)}\\ \mathbf{D} &= \begin{bmatrix}\Omega_{11}^{\Phi_{11}} & \Omega_{12}^{\Phi_{12}} & \Omega_{13}^{\Phi_{13}}\\ \Omega_{21}^{\Phi_{21}} & \Omega_{22}^{\Phi_{22}} & \Omega_{23}^{\Phi_{23}}\\ \Omega_{31}^{\Phi_{31}} & \Omega_{32}^{\Phi_{32}} & \Omega_{33}^{\Phi_{33}}\end{bmatrix}\end{aligned} \tag{20}$$

where the convenient tensor, $\mathbf{D}$ is later implemented in the damage rate tensor [26,27].

The damage rate tensor, $\dot{\boldsymbol{\omega}}$, is multiplicative superposition of the damage constant tensors, $\mathbf{B}$ and the convenient tensor, $\mathbf{D}$ using the elementwise Schur (or Hadamard) product as follows

$$\begin{aligned}\dot{\boldsymbol{\omega}} &= \mathbf{B}\circ\mathbf{D}\\ \mathbf{B}\circ\mathbf{D} &= \begin{bmatrix}B_{11}D_{11} & B_{12}D_{12} & B_{13}D_{13}\\ B_{21}D_{21} & B_{22}D_{22} & B_{23}D_{23}\\ B_{31}D_{31} & B_{32}D_{32} & B_{33}D_{33}\end{bmatrix}\end{aligned} \tag{21}$$

The damage rate tensor is coupled with the anisotropic creep strain rate equation defined as follows

$$\mathbf{e}^{cr} = A_{aniso}\tilde{\sigma}_{\text{Hill}}{}^{n_{aniso}}\frac{\mathbf{Ms}}{\sigma_{\text{Hill}}} \tag{22}$$

where A_{aniso}, n_{aniso} are secondary creep material constants found via creep tests, **M** is the Hill compliance tensor, **s** is the Cauchy stress vector, and $\tilde{\sigma}_{\text{Hill}}$ is the Hill equivalent (net) stress due to the effective stress tensor, $\tilde{\boldsymbol{\sigma}}$. To ease the implementation of the model into finite element code, the symmetric stress and strain tensors are converted back and forth to stress and strain vectors (e.g. $\tilde{\boldsymbol{\sigma}} \rightleftarrows \tilde{\mathbf{s}}$, $\boldsymbol{\varepsilon}^{cr} \rightleftarrows \mathbf{e}^{cr}$). Material rotation can be performed in the damage rate tensor as follows

$$\begin{aligned}\mathbf{b}^R &= M_{aniso}\sqrt{\mathbf{s}_p{}^T\mathbf{TMT}^T\mathbf{s}_p}\,\chi_{aniso}\frac{\mathbf{TM}_b\mathbf{T}^T\mathbf{s}_p}{\sqrt{\mathbf{s}_p{}^T\mathbf{TM}_b\mathbf{T}^T\mathbf{s}_p}}\\ \boldsymbol{\lambda}^R &= \phi_{aniso}\frac{\mathbf{TM}_\lambda\mathbf{T}^T\mathbf{s}_p}{\sqrt{\mathbf{s}_p{}^T\mathbf{TM}_\lambda\mathbf{T}^T\mathbf{s}_p}}\end{aligned} \tag{23}$$

and in the creep strain rate equation as follows

$$\mathbf{e}^{cr} = A_{aniso}\sqrt{\tilde{\mathbf{s}}^T\mathbf{TMT}^T\tilde{\mathbf{s}}}^{n_{aniso}}\frac{\mathbf{TMT}^T\mathbf{s}}{\sqrt{\mathbf{s}^T\mathbf{TMT}^T\mathbf{s}}} \tag{24}$$

where **T** represents a material orientation transformation tensor. The use of Hill compliance tensors provide a great method by which both the secondary and tertiary creep behavior of the material can be modeled under material reorientation.

To apply this model a fair number of constants are necessary. Six secondary creep constants need to be analytically determined and can be easily found via uniaxial creep tests (A_L, A_T, n_L, and n_T,). Using the Kachanov-Rabotnov formulation and an iterative optimization scheme, nine tertiary creep constants need to be numerically determined (M_1, M_2, χ_1, χ_2, ϕ_1,and ϕ_2). Lastly, three sets of six Hill constants need to be analytically determined for the **M**, $\mathbf{M}_b$, and $\mathbf{M}_\lambda$ Hill compliance tensors. The constant associated with the **M** tensor can be found through state of stress equivalence and material rotation of the creep rate Eq. (24). The constants for the $\mathbf{M}_b$ and $\mathbf{M}_\lambda$ Hill compliance tensors can be found through a similar method using the damage constant tensors Eq. (23). Stewart [28] has developed analytical solutions for the necessary constants.

Creep rupture time predictions can be easily obtained. Symbolic expansion of the damage rate tensor Eq. (21), provides the following

$$\dot{\boldsymbol{\omega}} = \begin{bmatrix} \dfrac{b_1}{(1-\omega_{11})^{\lambda_1}} & 0 & 0 \\ 0 & \dfrac{b_2}{(1-\omega_{22})^{\lambda_2}} & 0 \\ 0 & 0 & \dfrac{b_3}{(1-\omega_{33})^{\lambda_3}} \end{bmatrix} \tag{25}$$

where b_i (hr^{-1}) and λ_i are expressed in Eq. (17). Assuming that each term of damage is independent, component wise derivation provides

$$\begin{aligned} t_{r_i} &= \left[1-(1-\omega_{cr})^{\lambda_i+1}\right]\left[(\lambda_i+1)b_i\right]^{-1} \\ t_r &= \min\left\{t_{r_i}\right\} \\ i &= 1,2,3 \end{aligned} \tag{26}$$

where full vector predictions are produced. Rupture time, t_r, can be considered equal to the minimal component found in the $\mathbf{t_r}$ vector. Additionally, rupture time could be determined using some effective approach but this is left for future study. Critical damage is assumed to be equal to that found in the **ω** component where rupture is expected to occur. Additionally, the final direction of rupture can be estimated based on the critical damage tensor.

The strength of the improved anisotropic model is that it provides the ability to predict rupture time and/or critical damage for any state of stress or material orientation.

4. MATERIAL

Nickel-based superalloys are commonly used as turbine blade materials due to their strength, creep-resistance, and corrosion resistance at high temperature. Applying directional solidification techniques, it was discovered that grain boundaries could be minimized perpendicular to the principal load direction and improved rupture strength could be achieved [29]. The subject material is DS GTD-111, a dual-phase γ- γ' Ni-based superalloy derived from Rene' 80 [30].

The γ matrix phase is FCC austenitic Nickel (Ni), while the γ' precipitated phase is $L1_2$ structured nickel-aluminde (Ni_3Al) with a bimodal distribution [32,33]. Nickel (Ni), aluminum (Al), and chromium (Cr) impart oxidation resistance. The elements titanium (Ti) and molybdenum (Mo) increase the volume fraction of γ' precipitate particles. Titanium is used to control lattice mismatch and the formation of anti-phase boundary energy (APBE). Carbides to pin grain boundaries are formed of carbon (C) and Ti, W, Mo, Cr, and Ta. Chromium (Cr) raises hot corrosion resistance. The elements Cr, Mo, and W are solid solution strengtheners. Various secondary elements are utilized to impart increased ductility, workability, and castability.

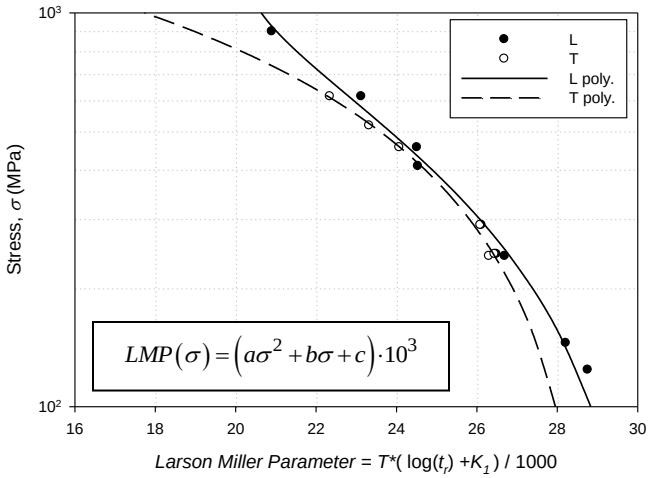

Figure 2 - Larson-Miller plot of stress versus the LMP parameter for DS GTD-111 for longitudinal (L) and transverse (T) specimen

Creep deformation experiments up to rupture were conducted on L and T-oriented specimen of DS GTD-111 according to an ASTM standard E-139 [34] for a range of temperature and stress conditions.

5. RESULTS

Using the Larson-Miller method with the K_1 constant equal to 20.07 and 19.86 for L and T-oriented specimen respectively, a plot of applied stress versus the calculated *LMP* parameter is produced found in Figure 2. The polynomial regression equation shown on Figure 2 is used to determine the *LMP* parameter at a set stress level. The terms of the polynomials for L and T orientations can be found in Table 1 with an R^2 value of 0.9914 and 0.96964 respectively. Larson-Miller creep rupture predictions are shown in Figure 3(a, b). It is observed that this method is fairly accurate in predicting the creep rupture of both L and T-oriented specimen. It produces an inverse parabolic curve for stress versus creep rupture time where as temperature increases the creep life is reduced.

Table 1 – *LMP* parameter polynomial terms for DS GTD-111 longitudinal (L) and transverse (T) specimen

Specimen	a	b	c
L	6.760E-06	- 1.655E-02	3.042E+01
T	- 8.822E-07	- 1.039E-02	2.900E+01

Table 2 - Monkman-Grant constants for DS GTD-111 longitudinal (L) and transverse (T) specimen [7]

Specimen	*m*	K_{MG}
L	0.89109	-0.99658
T	0.90463	-1.43048

Table 3 - Secondary creep constants of the Norton power law for DS GTD-111 longitudinal (L) and transverse (T) specimen

Temperature	*n*		*A*	
(°C)	L	T	L	T
649	8.500		5.909E-30	
760	7.591	10.890	1.393E-25	8.090E-35
816	7.000	9.650	2.477E-23	3.572E-30
871	6.507	6.516	5.764E-21	3.480E-21
940	6.000	4.850	3.507E-18	4.210E-16
982	5.547		8.290E-17	

Table 4 - Secondary creep regression terms for DS GTD-111 longitudinal (L) and transverse (T) specimen

	A_0	A_1	n_0	n_1
L	6.551E-56	9.207E-02	1.425E+01	- 8.839E-03
T	9.231E-118	2.507E-01	3.808E+01	- 3.555E-02

To implement the Monkman-Grant method, the *m* and K_{MG} constants need to be determined. Previous authors have produced these constants listed in Table 2 for DS GTD-111 for both longitudinal and transverse specimen [7]. It is desirable to replace the minimum creep strain rate in the Monkman-Grant relation with the Norton power law for secondary creep, Eq. (3). The *A* and *n* secondary creep constants for DS GTD-111 were determined at multiple temperature levels and are listed in Table 3. Minimum creep strain rate data suggests that DS GTD-111 does not exhibit an Arrhenius form of temperature-dependence; therefore, temperature-dependence is introduced in the following form

$$A(T) = A_0 \exp(A_1 T) \tag{27}$$

$$n(T) = n_1 T + n_0 \tag{28}$$

where A_0, A_1, n_0, and n_1 are constants found in Table 4 and *T* is in units Celsius. The Monkman-Grant relation, Eq. (9), is rewritten into the following form

$$\log(t_r) + m\log\left[A(T)\cdot\sigma^{n(T)}\right] = k_{MG} \tag{29}$$

Now the stress and temperature-dependence of the minimum creep strain rate is accounted for within the Monkman-Grant relation. Monkman-grant creep rupture predictions are shown in Figure 3(c, d). This method accurately predicts the creep rupture behavior for both L and T-oriented specimen. It produces a negative sloped linear curve for stress versus creep rupture time (on a log-log scale) where as temperature increases the creep life is reduced.

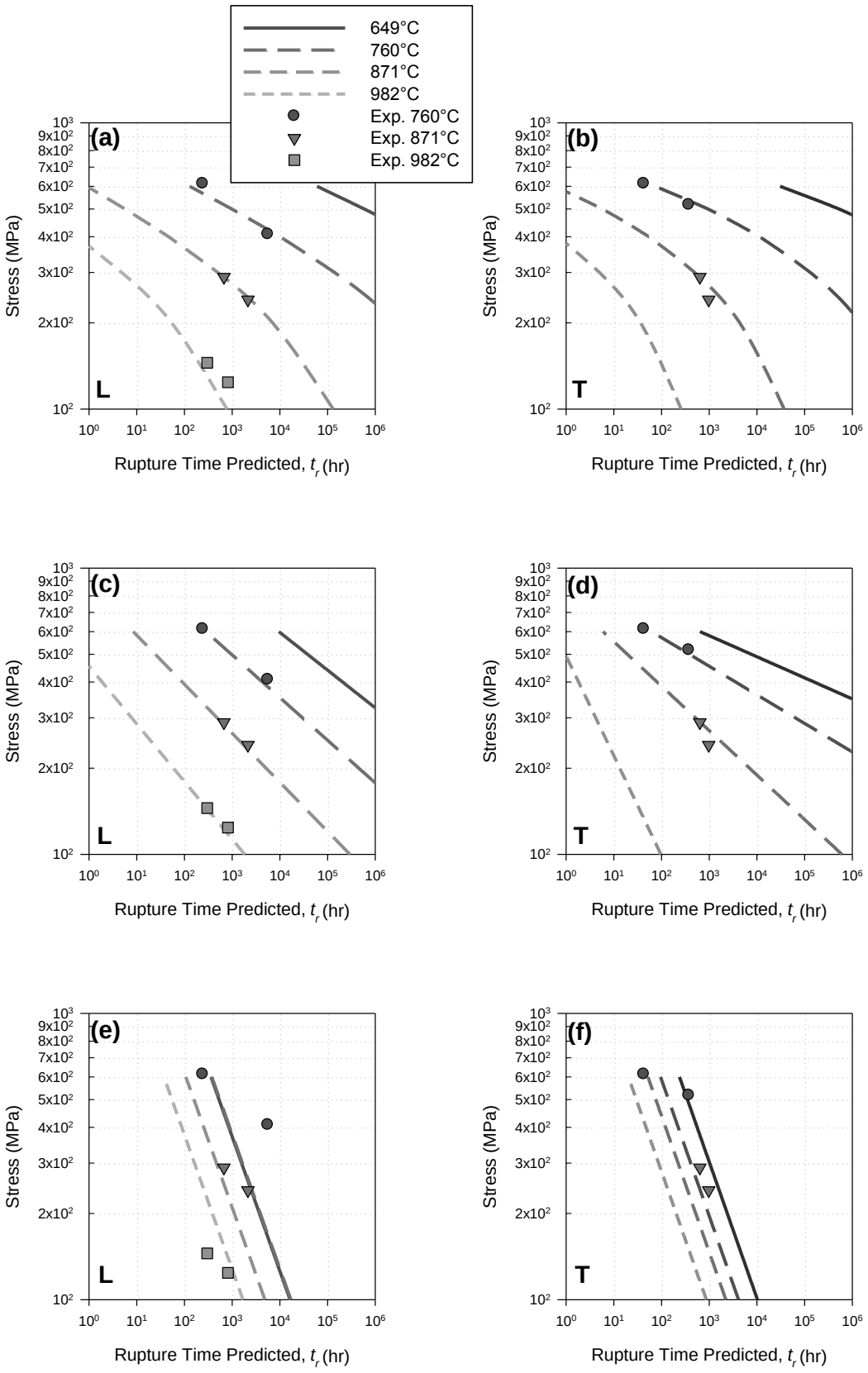

Figure 3 - Creep rupture predictions of (a, c, e) L and (b, d, f) T-oriented DS GTD-111 at various temperatures using (a, b) Larson-Miller (c, d) Monkman-Grant (e, f) and Kachanov-Rabotnov methods

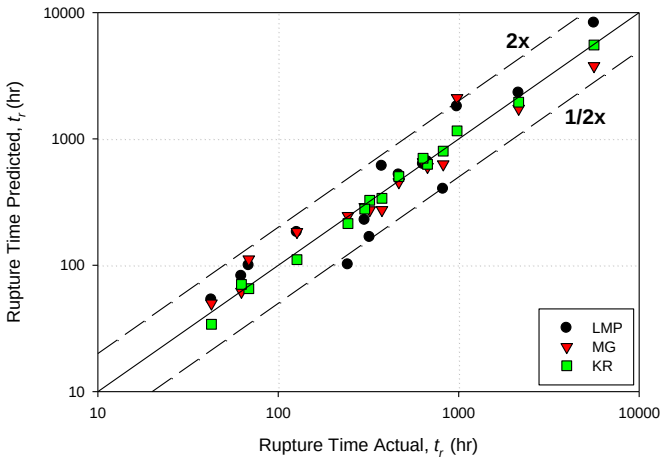

Figure 4 - Predicted creep rupture life of DS GTD-111 using the Larson-Miller (LMP), Monkman-Grant (MG), and Kachanov-Rabotnov (KR) methods

Table 5 - Tertiary creep damage constants for DS GTD-111

	Temperature (°C)	Stress (MPa)	M $(MPa^{-\chi}hr^{-1})$x10^{-11}	χ	ϕ
L	649	896	10.0	1.880	55.000
L	760	408	20.9	1.900	8.500
L	760	613	19.8	2.231	13.261
T	760	517	36.2	2.106	14.810
T	760	613	51.8	2.203	39.931
L	816	455	64.1	2.257	3.792
T	816	455	167.6	1.981	28.224
L	871	241	96.0	2.022	7.161
L	871	289	131.0	2.054	9.698
T	871	241	263.0	2.098	2.296
T	871	289	345.8	1.919	6.823
L	940	244	579.1	2.310	7.069
T	940	244	600.0	2.290	7.069
L	982	124	655.9	2.221	3.278
L	982	145	665.2	2.288	5.126

Table 6 - Tertiary creep damage exponent ϕ polynomial terms for DS GTD-111

	ϕ_3	ϕ_2	ϕ_1	ϕ_0
L	-5.124E-06	1.338E-02	-1.161E+01	3.354E+03
T	5.826E-04	-1.128E+00	5.502E+02	0.0

Table 7 - Hill's Compliance tensor constants for DS GTD-111

Tensor	F	G	H	L	M	N
$\mathbf{M}$	0.5	0.5	0.387	1.641	1.641	1.273
$\mathbf{M}_b$	0.5	0.5	0.643	1.051	1.051	1.785
$\mathbf{M}_\lambda$	0.5	0.5	-5.08E-3	9.071	9.071	0.490

To implement the Kachanov-Rabotnov formulation, the tertiary creep damage constants M, χ, and ϕ need to be determined. Previous research by the authors has demonstrated that the constants can be determining through optimization using a finite element package and compare simulated results with experimental using a least squares objective function. The global simulated annealing optimization routine produce the constants listed in Table 5. The constants M and ϕ exhibit temperature-dependence while the constant χ does not. The temperature-dependent equations for the tertiary creep damage coefficient, M, is assumed as follows

$$M(T) = \lambda_1 M_1 \exp(\lambda_2 M_0 T)$$
$$\begin{pmatrix}\mathbf{L}\\ \mathbf{T}\end{pmatrix} orientation = \begin{cases} \lambda_1 = \lambda_2 = 1 \\ \lambda_1 = 0.8245, \lambda_2 = 1.0722 \end{cases} \quad (30)$$

where T is in unit Celsius and M_1 $(MPa^{-\chi}hr^{-1})$ and M_0 (unitless) are constants found to be 6.62736E-04 and 5.4645E-04 ,respectively. The temperature-dependent functions for the tertiary creep damage coefficient, M, carry an R^2 value of 0.9593 and 0.9409 for L and T-oriented specimen, respectively. The unitless weight values λ_1 and λ_2, were used to implement the formulation for both L and T orientations. The tertiary creep damage exponent, ϕ, was found to produce a less than ideal fit to temperature in a polynomial equation of the form

$$\phi(\sigma) = \phi_3 T^3 + \phi_2 T^2 + \phi_1 T + \phi_0 \quad (31)$$

where T is in units Celsius, and ϕ_0, ϕ_1, ϕ_2, and ϕ_3 are constants found in Table 6. The tertiary creep damage exponent, χ (unitless), was found to exhibit no temperature-dependence and was set to the average value for longitudinal and transverse specimen observed as 2.1292 and 2.0994, respectively. The tertiary creep damage exponent, χ, is highly stress sensitive; therefore, small changes have a significant effect on rupture time predictions. Bonora and Esposito have demonstrated that when using the power law structure the creep exponent varies with stress [35]. The available optimized constants were based on a per-specimen optimization; therefore, the best constants for a set temperature at any applied stress level were not obtained. This severely limits the accuracy of the Kachanov-Rabotnov constants used in this paper. Kachanov-Rabotnov creep rupture predictions are shown in Figure 3(e, f). It is observed that predictions do not correlate with experimental data. It should be noted that when the optimized constants are directly applied (instead of using temperature-dependent functions),

the rupture time predictions are highly accurate. It is the authors' suggestion that in future study batch optimization be performed to produce a globally optimized set of tertiary creep damage constants.

A comparison of the creep rupture predictions using Larson-Miller, Monkman-Grant, and the Kachanov-Rabotnov formulation is provided in Figure 4. It is observed that in most cases the rupture time predictions are within a factor of two. Of the three methods, Monkman-Grant can be considered the easiest to implement due to the small number of constants needed to produce a fairly accurate prediction. It would be particular useful for isotropic materials where creep mechanism are not orientation-dependent. Due to the limited accuracy of the Kachanov-Rabotnov tertiary creep damage constants in temperature-dependent form, the actual optimized constants are directly used in the current figure. The figure demonstrates the potential accuracy of the Kachanov-Rabotnov if batch optimization was conducted.

To implement the new transversely-isotropic formulation, the same tertiary creep damage constants necessary for the Kachanov-Rabotnov formulation are need for L and T-oriented specimen as well as eighteen analytically derived constants for the three Hill's compliance tensors. Only one set of creep rupture test at an equivalent 289MPa and 871°C for L, and T-oriented specimen is available. The tertiary creep constants for the L and T specimen at 289MPa and 871°C are found in Table 5.

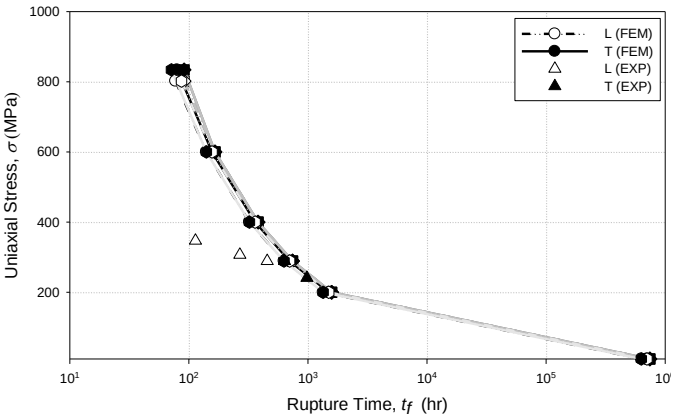

Figure 5– Stress-rupture time curves for DS GTD-111 for L and T-oriented specimen at 871°C with (a) unaixial – circle (b) biaxial – square , (c) pure shear – diamond , and (d) triaxial – hex

The Stewart [28] analytical solution to the Hill's compliance tensor constants was used and values are listed in Table 7. The Rupture time predictions using the transversely-isotropic formulation regresses to the Kachanov-Rabotnov prediction for L and T-oriented specimen.

6. PARAMETRIC STUDY

The strength of the new transversely-isotropic formulation is that any complex stress state and material orientation can be applied. To demonstrate, predictions of rupture time for uniaxial, biaxial, pure shear, and triaxial states of stress were applied for L and T-oriented specimen at 871°C at equal levels of equivalent stress. A plot of the stress against rupture time can be observed in Figure 5. Pure shear was found to produce the shortest rupture times while triaxial the longest. This is due to the loading conditions being based around von Mises equivalent stress instead of the internally used Hill's equivalent stress. This should be corrected in later studies. For all loading conditions, and at each material orientation (L and T), the maximum load applied was equal to material ultimate tensile strength (UTS). At every instance a rupture time prediction was found at less than 200 hrs. Under UTS equivalent loading the rupture time should be minimal and related to ductile necking until rupture. Additional creep tests should be performed at the UTS in L and T-oriented specimen to determine the short time before failure. A potentially useful property of the new transversely-isotropic rupture time prediction equation is that it provides a method by which specimen rupture time can be predicted for conditions which may have been determined under purely elastic loading. When it is necessary to conduct multiple tests and available lab experiment time is limited it can be used to accurately predict the rupture time of specimen for alternative states of stress.

7. CONCLUSION

The Larson-Miller, Monkman-Grant, and Kachanov-Rabotnov formulation are all shown to produce viable rupture time predictions. It was determined that the Monkman-Grant method is the easiest to implement and should be selected when dealing with isotropic materials. The Kachanov-Rabotnov formulation is shown to require tertiary creep constants that are determined through batch optimization. The new transversely-isotropic formulation is found to produce the same creep rupture time predictions as the Kachanov-Rabotnov formulation for L and T-oriented specimen. It is able to determine the creep rupture time for any arbitrary material orientation. The parametric study demonstrates that it is able to predict the approximately the same creep rupture time for uniaxial, biaxial, pure shear, and triaxial state of stress at an equal value of von Mises equivalent stress. In future work, batch optimization will be performed to produce more suitable tertiary creep damage constants. Additional L and T-oriented test will be conducted at equal levels of applied uniaxial stress.

8. ACKNOWLEDGEMENTS

Calvin Stewart is thankful for the support of a Mcknight Doctoral Fellowship through the Florida Education Fund.

REFERENCES

[1] Xie, Y., Wang, M., Zhang, G., and Chang, M., 2006, "Analysis of Superalloy Turbine Blade Tip Cracking During Service," *Engineering Failure Analysis*, **13**(8), pp. 1429-1436.
[2] Pridemore, W. D., 2008, "Stress-Rupture Characterization in Nickel-Based Superalloy Gas Turbine Engine

Components," *Journal of Failure Analysis and Prevention*, **8**(3), pp. 281-288.
[3] National Research Council (U.S.) Committee on Materials for Large Land-Based Gas Turbines, 1986, "Materials for large land-based gas turbines," National Academy Press.
[4] Larson, R. and Miller, J., 1952, *Trans. ASME*, **74**, pp. 765.
[5] Viswanathan, R., 1989, "Damage Mechanisms and Life Assessment of High-Temperature Components", *ASM International*, pp. 65-67.
[6] Nomoto, A., Yaguchi, M. and Ogata, T., 2000, "Study on Creep Properties and Microstructural Relation in Directionally Solidified Nickel Base Superalloy", *Key Engineering Materials*, Vols. 171-174, pp. 569-576.
[7] Ibanez, A. R., Srinivasan, V. S., and Saxena, A., 2006, "Creep Deformation and Rupture Behaviour of Directionally-solidified GTD 111 Superalloy," *Fatigue & Fracture of Engineering Materials & Structures*, **29**(12), pp. 1010 – 1020.
[8] Norton, F. H., 1929, *The creep of steel at high temperatures*, McGraw-Hill, London.
[9] Hill, R., 1950, *The Mathematical Theory of Plasticity*, Oxford University Press, New York.
[10] Hyde, T. D., Jones, I.A., Peravali, S., Sun, W., Wang, J.G., and Leen S. B., 2005, "Anisotropic Creep Behavior of Bridgman Notch Specimens," *Proceedings of the Institution of Mechanical Engineers, Part L: Journal of Materials: Design and Applications*, **219**(3), pp. 163-175.
[11] Dorn, J.E., 1955, "Some Fundamental experiements on high temperature creep", *Journal of the Mechanics and Physics of Solids*, **3**, pp. 85-116.
[12] Monkman, F. and Grant, N., (1956), Proc. ASTM, **56**, p. 595.
[13] Guo, J., Yuan, C., Yang, H., Lupinc, V and Maldini, M., (2001), "Creep-Rupture Behavior of a Directionally Solidified Nickel-Base Superalloy", Metallurgical and Materials Transactions A, **32**, pp. 1103-1110.
[14] Kachanov, L. M., 1967, *The Theory of Creep*, National Lending Library for Science and Technology, Boston Spa, England, Chaps. IX, X.
[15] Rabotnov, Y. N., 1969, *Creep Problems in Structural Members*, North Holland, Amsterdam.
[16] Leckie, F. A., and Hayhurst, D. R., 1977, "Constitutive equations for creep rupture," *Acta Metall.*, **25**, pp. 1059 – 1070.
[17] Leckie, F. A., and Ponter, A., 1974, "On the State Variable Description of Creeping Materials," *Ing.-Archiv.*, **43**, pp. 158-167.
[18] Hayhurst, D., Trampczynksi, W., and Leckie, F. A., 1980, "Creep Rupture and Nonproportional Loading," *Acta Metall.*, **28**, pp 1171-1183.
[19] Hyde, T.D., Sun, W., and Williams, J.A, 1999, "Creep Behaviour of Parent, Weld and HAZ Materials of New, Service-Aged and Repaired 1/2Cr1/2Mo1/4V: 2 1/4Cr1Mo Pipe Welds at 640°C," *Material at High Temperatures*, **16**(3), pp 117-129.
[20] Maclachlan, D. W. and Knowles, D. M., 2000, "Creep-Behavior Modeling of the Single-Crystal Superalloy CMSX-4," *Metallurgical and Materials Transactions A*, **31**(5), pp. 1401-1411.
[21] Batsoulas, N. D., 2009, "Creep Damage Assessment and Lifetime Predictions for Metallic Materials under Variable Loading Conditions in Elevated Temperature Applications," *Steel Research International*, **80**(2), pp 152-159.
[22] Odquist, F., and Hult, J., 1962, *Kriechfestigkeit metallischer Werkstoffe*, Springer Berlin.
[23] Murakami, S. and Ohno, N., 1981, "A Continuum Theory of Creep and Creep Damage.," *In Creep in Structures*, A. R. S. Ponter and D. R. Hayhurst, eds., pp. 422–443.
[24] Altenbach H., Huang C., and Naumenko K., 2002, "Creep damage Predictions in Thin-Walled Structures by use of Isotropic and Anisotropic Damage Models," *Journal of strain analysis for engineering design*, **37**(3), pp. 265-275.
[25] Murakami, S. and Sanomura, Y., 1985, "Creep and Creep Damage of Copper Under Multiaxial States of Stress," *In Plasticity Today*, edited by A. Sawczuk and G. Bianci, pp. 535–551.
[26] Schur, I., Joseph, A., Melnikov, A., and Rentschler, R., 2003, *Studies in memory of Issai Schur*, Springer, Chap. xci.
[27] Bernstein, D. S., 2005, *Matrix mathematics*, Princeton University Press, pp 252-253, Chap. 7.3.
[28] Stewart, C. M., 2009, "Tertiary Creep Damage Modeling of a Transversely Isotropic Ni-Based Superalloy" Master's Thesis, University of Central Florida, Orlando, Fl.
[29] Viswanathan, R., and Scheirer, S. T., 2001, "Materials Technology for Advanced Land Based Gas Turbines," *Creep: proceedings of the international conference on creep and fatigue at elevated temperatures*, Tsukuba, Japan, No.01-201 (20010603), pp. 7-21.
[30] Li, L., 2006, "Repair of directionally solidified superalloy GTD-111 by laser-engineered net shaping," *Journal of Materials Science*, **41**(23), pp. 7886-7893.
[31] Schilke, P. W., Foster, A.D., Pepe, J. J., and Beltran, A. M., 1992, "Advanced Materials Propel Progress in LAND-BASED GAS TURBINES," *Advanced Materials and Processes*, **141**(4), pp. 22-30.
[32] Gordon, A. P., 2006, "Crack Initiation Modeling of a Directionally-Solidified Nickel-Base Superalloy," Dissertation, *Georgia Institute of Technology*, pp. 6-59.
[33] Gale, W. F., Smithells, C. J., and Totemeier, T. C., 2004, *Smithells Metals Reference Book 8th Edition*, Butterworth-Heinemann, pp. 7-12, Chap. 38.
[34] ASTM E-139, "Standard Test Methods for Conducting Creep, Creep-Rupture, and Stress-Rupture Tests of Metallic Materials," No. 03.01, West Conshohocken, PA.
[35] Bonora, N., and Esposito, L., 2008, "Mechanism Based Unified Creep Model Incorporating Damage," *Proceedings of the ASME 2008 Pressure Vessels and Piping Conference (PVP2008)*, PVP2008-61034, pp. 1189-1193 , Chicago, IL, July 27-31.